15.315

MICROBURST DETECTION WITH NEXRAD AMDA†

Mark S. Veillette, Betty J. Bennett,
Margo Pawlak, Robert Frankel
MIT Lincoln Laboratory, Lexington, MA
September, 2013

1. INTRODUCTION

Microbursts (or downbursts) are areas of strong, divergent and often damaging winds which are caused by sudden convective downdrafts (Figure 1), see (Fujita, 1976). The regions of wind shear generated by the outflow of a microburst pose a danger to aviation and civilians, particularly at lower altitudes. Pilots who encounter divergent shear experience an initial spike in head wind followed by a sudden shift to tail wind after passing through the center of the outflow. This, combined with the force of the downdraft, causes a serious hazard at low altitudes. There are forty-six (46) major airports that currently rely on automated wind shear detection provided by the Integrated Terminal Weather System (ITWS) which processes TDWR data, (Evans & Ducot, 1994), (Wolfson et al. 1994). Another thirty-five (35) medium-sized airports are protected by the ASR-9 Wind Shear Processor (WSP) (Newell & Cullen, 1994). However, there are still many medium-sized and smaller airports that could benefit from wind-shear protection but did not meet cost benefit thresholds. In this paper, the Automated Microburst Detection Algorithm (AMDA) developed for the WSR-88D (henceforth, NEXRAD) is presented. The larger coverage of the NEXRAD network, combined with AMDA may provide a cost effective way to provide new wind shear and microburst detection coverage to a broad set of airports and the potential for

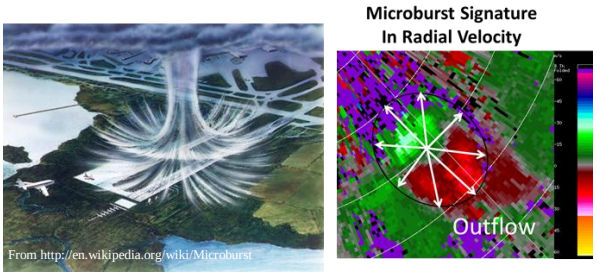

Figure 1: *Powerful storms are capable of generating "microbursts", which are sudden downdrafts that cause strong divergent winds near the surface (left). When viewed in radar data, these events often create the green-to-red couplet present in the image on the right. This pattern represents wind blowing towards the radar (green) transitioning quickly to wind moving away from the radar (red) which is the radial projection of the outflow shown in white.*

enhanced coverage at high impact airports (Hallowell, 2009).

AMDA is not a new algorithm; it first appeared as a part of the ASR-9's WSP. AMDA was originally based on the TDWR microburst detection algorithm, but has since evolved to account for strengths & weaknesses of other platforms. In this present work, AMDA was upgraded and tuned for NEXRAD inputs and is scheduled to be released as part of the Open Radar Product Generator (ORPG) (Jain, et al. 1997) in the near future.

Other microburst and wind shear detection systems have been developed over the years, see for instance (Albo, 1994) or (Dance et al. 2002). Most notably, there was the Damaging Downburst Prediction and Detection Algorithm (DDPDA), (Smith et al. 2004) which was also developed for NEXRAD. Similar to AMDA, this algorithm provides detection capability. However, there are a number of features which set these two apart.

Corresponding Author: Mark S Veillette, MIT Lincoln Laboratory, 244 Wood Street, Lexington, MA 02420
e-mail: mark.veillette@ll.mit.edu

†This work was sponsored by the Federal Aviation Administration (FAA) under Air Force Contract FA8721-05-C-0002. Opinions, interpretations, conclusions, and recommendations are those of the author and are not necessarily endorsed by the United States Government.

As its name suggests, the DDPDA was developed primarily as a prediction tool. The DDPDA focuses mainly on wet microbursts. Also, the algorithm relies on the Storm Cell Identification and Tracking (SCIT) Algorithm (Johnson et al. 1998). In contrast, AMDA is designed to detect both wet and dry microbursts, and does not rely heavily on other algorithms.

While is it universally agreed that a microburst is an area of divergent winds at the surface generated by a convective downdraft, there is slight disagreement about the *precise* definition of a microburst across the literature. Different definitions are set apart by the magnitude and time scale of the wind shear generated by a downdraft (this point is discussed further in (Trobec, 2006)). There are a number of "rules of thumb" for identifying wind shear signatures in radar data (Brown & Wood, 2006), however labeling events as "true" microbursts in practice remains a challenge even for experienced meteorologists. Several researchers define a microburst by applying a threshold to the velocity loss across a pattern of divergent wind at the surface. For example, (Wilson et al. 1984) and (Knupp, 1989) use a threshold of 10 m/s or greater in the surface scan, while (Wolfson et al., 1994) use 15 m/s or greater. In (Fujita, 1985), microbursts were further classified by size, where a microburst is defined to have radius < 4km, while anything larger was called a "macroburst". For the development of AMDA, a microburst is defined as a region of which shear which exceeds 15 m/s velocity loss, and also has a radius less than 2 km. Larger events will be considered macrobursts to be consistent with Fujita's definition. Because of the infrequent scanning strategy of NEXRAD and since AMDA is to be used as a real-time tool, the time duration of the event is not factored into its definition of microburst.

In this paper, an overview of AMDA is provided. First, the components of the algorithm used to generate detections are described in detail. Then, AMDA's performance is assessed using two verification techniques.

2. ALGORITHM DESCRIPTION

AMDA is designed to detect divergent wind shear at the surface. It derives its detections from the NEXRAD radial velocity (V) and reflectivity (dBZ) data. The most important inputs are the 0.5^{o} base elevation of these products. If available, the 250m / 0.5^{o} super resolution (super-res) version of the base elevation data are used; however AMDA will still run on the coarser resolution data if super-res data are not available. In standard Volume Coverage Patterns (VCP), there is one base elevation received per volume scan and as a result, AMDA will generate one output product per volume after the base elevation is received. This amounts to approximately one product every 4 minutes at the fastest VCP. AMDA also ingests higher elevation data for generating volume products (see below), though these are optional inputs not required for AMDA to run.

It is worth noting some of the differences between the NEXRAD version of AMDA and its predecessor which was run on the ASR-9 WSP platform. Because of less frequent surface scanning of NEXRAD, additional image processing techniques were added to create more reliable radial shear segments and cluster formation (image filtering and utilization of radial shear, described below). In addition, volume products are created that process information from higher elevation scans to assist in validating shear segments. Significant parameter tuning and algorithm modifications were also required since NEXRAD AMDA is configured to use super-res base elevation data that has a higher angular resolution (720 0.5^{o} azimuthal sectors on NEXRAD compared to 256 1.4^{o} sectors on the ASR-9).

The steps AMDA takes to create detections are shown in Figure 2. The volume products are updated after receiving data for each elevation, and the rest of AMDA is run upon receiving a base elevation input of reflectivity and velocity. The main component of AMDA is comprised of two parts, generating interest, and generating

detections. These are described in more detail below.

2.1 Generating Volume Products

AMDA has the option to process all incoming elevation angles of dBZ and V and generate specialized volume products used later in the algorithm. The two volume products currently generated are Vertically Integrated Liquid (VIL) and the center of mass height of reflectivity. Both of these features were observed as important precursors to powerful downdrafts in the development of the DDPDA. After a required number of elevations are ingested, VIL is computed by converting incoming reflectivity values to liquid water content, and then integrating over vertical columns. The width of the vertical column is an adjustable parameter. The center of mass field is constructed using the height of reflectivity observations greater than a parameterized threshold (typically 20 dBZ). Fields are linearly interpolated between radar observations at various altitudes, and data are discarded if they become too old.

2.2 Generating Interest

The interest generation step in AMDA is used to detect patterns and signals associated with microbursts and wind shear which are present in reflectivity and velocity data. This information is used downstream in AMDA for generating shear segments and for creating detections. In the interest generation module, a number of image processing steps are applied to the input images to generate two images: Radial Shear and Reflectivity Interest as seen in Figure 2.

Radial shear is obtained by applying a least square filter to radial velocity data in polar form. The window size used for the least square filter is a parameter. The units of radial shear are (m/s)/m = s^{-1} and represent the change in radial velocity as one moves outward along a radial. This field highlights regions with increasing radial velocity which are associated with divergent shear. Since the least square filter is sensitive to outliers and noisy data, a median filter is applied to the incoming radial velocity data before processing. If the computation window does not contain enough valid pixels, or the correlation coefficient computed during the least squares fit is too low, the value of radial shear is set to a null value.

To create Reflectivity Interest, AMDA uses a pattern recognition technique called 2D Functional Template Correlation (FTC), (Delanoy, 1992). FTC is used in a number of “detectors” to extract features from the base reflectivity image. The detectors currently used in AMDA are described below. Not all detectors are required to run AMDA, but it is recommended to run with at least two. Each detector is configured using an external parameter file.

Absolute Reflectivity Detector: This detector is designed to return an interest map of where precipitation is the strongest, which is useful for detecting locations of potential wet microbursts. A 5x5 FTC is applied to the base reflectivity and the resulting image is eroded. Areas that have no valid weather are set to zero.

Relative Peaks Detector: Drier microbursts and wind shear may not show sufficient reflectivity to be detected by the Absolute Reflectivity Detector. For this reason, AMDA also uses a detector which looks for regions of *relative* maxima or “peakiness” in the reflectivity. This brings out weaker storm cores which are characteristic of dry microbursts. The detector works by subtracting a smoothed reflectivity image from the original reflectivity and then applying an FTC on the difference to detect positive regions. This process is repeated using two different sized Gaussian kernels to detect structures of different scales. The maximum peakiness detected over both sized kernels is used as the result, and where there is no valid weather the result is set to 0.

Zero Crossing Detector: The zero line can sometimes cause the segment generation algorithm to detect divergence that is not actually present. This zero crossing detector is designed

to inhibit detection of segments where there is a zero line in velocity due to the radial alignment of the winds to the radar beam. This detector acts as a "negative" interest field to avoid false alarms.

VIL Detector: VIL detects reflectivity that might be present aloft and has not yet reached the surface. This detector maps an incoming VIL image generated in the volume generator to another input used to create Reflectivity Interest. No FTC is done in this step. Incoming VIL is rescaled so it can be used to create the final interest image.

Center of Mass Height Detector: In addition to VIL, the height of the center of mass of all reflectivity surpassing a fixed threshold (20 dbz) is computed in the volume generator. This field locates reflectivity cores aloft in the volume scan prior to the velocity surface scan. This is another piece of supporting evidence for microburst onset. Similar to VIL, no FTC correlation is performed in this step.

Interest Field Generation: Each detector described above generates a field with values between 0-255 to be used for creating the final interest image. The fields Absolute Reflectivity (I_A), Relative Reflectivity (I_R), Zero Crossing (I_Z), VIL (I_V) and Center of Mass (I_C) are combined pixel-wise using a fuzzy logic combination:

$$I = \sum_{k=A,R,Z,V,C} W_k I_k \Big/ \sum_{k=A,R,Z,V,C} W_k.$$

The weights W_k in this combination are not simply fixed constants, rather they are themselves functions of the images I_k. For example, this weight function might be set so that if I_k is 128 (neutral) at a particular pixel, the weight W_k assigned at that pixel is 1.0. However if I_k is 255, the weight is set to 2.5. The weight functions are also specified in an external parameter file.

2.3 Generating Detections

After interest generation, the next step is to create shear segments and form detections. The steps for doing this are outlined in the rightmost panel of Figure 2. This section provides additional detail about each of these steps. Each sub process has a number of parameters which define various thresholds referred to below.

Generate Shear Segments: In this process, each radial of the base velocity is scanned to create segments of divergent wind shear. This step combines the Radial Shear field and a signal processing algorithm applied to each radial individually. The start of a segment is located by searching for an increase in velocity between two gates. The segment then continues along the gates of the radial until one of the following occurs:

(i) The radial ends
(ii) Too many missing velocity values are encountered
(iii) Too many pixels with a radial shear below a threshold are encountered
(iv) The total velocity decrease measured along the segment is too high
(v) Too many large increases are detected

Conditions (iv) and (v) are used to account for noisy signals as it allows for small decreases in the velocity to be ignored and for erroneous increases that skew the radial shear to be discarded. Segments that fail to meet a length requirement or a minimum velocity loss (maximum velocity difference across the entire segment) are discarded. Segments that are too long are broken into smaller segments.

Cluster Segments: After shear segments are formed, each segment is "validated" using the Reflectivity Interest image. If the sum of interest values along a segment fails to meet a threshold, the segment is discarded. The remaining segments are clustered into initial "alarms". This is done by looping over all segments and checking if a segment overlaps the midpoint of a segment already in a cluster (segments which are not part of another cluster start a new cluster). Once all clusters have been formed, a number of cluster features are computed, including strength (maximum velocity loss), area, range, and maximum radial wind speed. Clusters that fail to meet a size and strength threshold are discarded.

Clusters that are too large are broken into smaller clusters.

Assimilate Evidence: After clusters are created, further checks are done before deciding whether to keep or to discard the cluster. AMDA attempts to classify each cluster into one of the following four categories:

1. *Wind-Shear*: Regions of divergent shear whose strength is less than 15 m/s and diameter is larger than 2km.
2. *Microburst:* A region of shear with strength greater than 15 m/s and radius less than 2km.
3. *Macroburst*: A region of shear with strength greater than 15 m/s and radius greater than 2km.
4. *Speed Shear* ("Travelling Microburst"): A microburst or macroburst where the sign of the radial velocity does not change within the cluster.

All thresholds listed here are adjustable parameters. If a cluster does not fall into any category listed here, it is discarded.

Generate Shapes: Finally, the remaining segment clusters are turned into "band-aid" shapes to represent the output detections. Band-aid shapes were chosen for consistency because these shapes are currently used on the ITWS display for showing wind shear detections.

3. ALGORITHM ASSESMENT

The next step in this process is to ensure that detections output by AMDA adequately depict regions of dangerous wind shear. This section will look at a sample of AMDA output, and attempt to verify AMDA output using different techniques.

3.1 Algorithm Examples

We will begin by viewing algorithm output in a few selected cases where there was wind shear present. Figure 3 shows the application of AMDA to four different cases. These cases include a mixture of microbursts, macrobursts, and other less severe wind shear detections.

Each cell of Figure 3 shows base reflectivity on the left and radial velocity on the right. The white shapes represent detections generated by AMDA. The number in white on the radial velocity image represents the velocity loss in units of m/s. Any strength measurement greater than 15 m/s represents a "severe" event (microburst or macroburst), whereas events with strength less than 15 m/s are considered wind shear alerts.

The top image in Figure 3 shows a pair of cells generating microbursts with approximate strengths of 39 m/s and 15 m/s. A wind shear alert is also present to the east, with strength of 13 m/s. In the second image of Figure 3, a macroburst with strength 19 m/s is detected along with a smaller wind shear alert. Also present at this time was a weak tornado signature slightly west of the macroburst (It is possible, but unknown, if the outflow of the macroburst is related to the formation of the tornado).

In the bottom image of Figure 3, AMDA detects a macroburst east of the radar. In this case, the size of the region was large enough for AMDA to break a single macroburst detection into two overlapping detections. This is common for larger outflows such as this. Breaking up detections into smaller, possibly overlapping pieces is done to ensure single detections don't grow too large. Also, giving strength measurements at multiple points along a region gives a more detailed analysis of the event. Overlapping detections, or detections which occur close to each other, should not always be interpreted as separate events, but rather as multiple descriptions of the same event.

3.2 Objective Algorithm Verification Techniques

Unfortunately, there is no universal "truth" that can be used for objectively scoring microburst detections in terms of "Hits", "Misses" for "False Alarms". However, there are a number of ways to create approximate truth sets that can be used to

score AMDA. In this study, we used two independent methods of creating "truth" to perform this verification.

The first method scores AMDA using "human truth". In this method, a person was trained to identify wind shear patterns in radial velocity and reflectivity data from NEXRAD. A number of "events" were chosen for scoring, and the sequence of reflectivity and radial velocity images were shown to the human scorer. The scorer encircled "truth regions" of divergent shear, and recorded the observed maximum strength (velocity loss) and maximum recorded wind speed across each event. The observer was not shown AMDA detections during this process.

For scoring, detections are matched based on shape overlap for each scan. An AMDA detection that overlaps truth regions encircled by the observer are labeled a "match" and the difference in strengths is noted. A "hit" is recorded if the AMDA detection and its matching truth region had strengths greater than 15 m/s. Any detection with strength greater than 15 m/s with no match, or with a match of strength less than 15 m/s, is counted as a false alarm. A truth object with strength larger than 15 m/s that has no overlapping AMDA detection is counted as a "miss". An error margin of 2 m/s was allowed for detections with strength near 15 m/s (so for example, an AMDA detection with strength 16 m/s matched to a truth region with strength 14 m/s still counts as a "hit").

The "human truth" method generates truth data that are highly reliable. Moreover, this data can easily be compared to AMDA output because they are generated from the same data. However, this method also has some weaknesses. Generating human truth sets is time consuming, and hence only a relatively small number of events can be scored. Second, the human truth can only "see" detections captured by the infrequent scanning of NEXRAD. If a microburst occurs in between scans, or generates too weak a signal, it will not be recorded by either AMDA or the human scorer.

To make up for some of the short comings of the human truth method, a second verification technique was also used. This method uses output from the microburst detection algorithm running on ITWS (called MBDetect). These detections were received from the John A. Volpe National Transportation Systems Center live feed over the summers of 2012 and 2013 (http://www.volpe.dot.gov/). MBDetect has the advantage of more frequent scan times compared to NEXRAD AMDA, which makes ideal as a second form of "truth" that can be used to verify AMDA detections.

While there are a number of benefits of using ITWS as truth for AMDA, one should not look at an "apples to apples" comparison of the two sets of detections without being aware of several issues. First, there are a limited number of sites where AMDA coverage (60 km from each NEXRAD) overlaps the microburst detection range of MBDetect (35 km from each TDWR). When coverage overlap does exist, the distance between both radars causes storms to be seen at different angles and at different elevations in the atmosphere. This can affect the strength and location of a detection. In addition, the radars scan at different times, so if winds are rapidly changing, the results of the two algorithms might differ. Finally, MBDetect is not perfect, and is capable of generating false alarms and misses which negatively impact AMDA's score. To help address some of these issues, a "fuzzy" scoring method was developed that allows for limited differences in the exact location, timing and strength of AMDA detections when being compared to ITWS detections (time within 2 minutes, center location within 5 km, and strength within 5m/s).

3.3 Objective Algorithm Verification Results

The NEXRAD site chosen for the "human truth" scoring method was Little Rock, AR (KLZK). This is an example of a site that does not have TDWR coverage and could benefit from the automated wind shear detection provided by AMDA. Data for a number of "events" were run through AMDA,

and the results were compared to events identified by the human scorer. In all, there were over 200 AMDA detections scored in this process.

Figure 4 shows a comparison between the strength measurement of AMDA and the human recorded strength for all matches (non-matched detections are not shown, but these are counted in the POD/FAR statistics). This result shows a strong relationship between AMDA and human truth. By looking at the proportion of hits, misses and false alarms, the Probability of Detection (POD = hits / (hits + misses)) is 98.7%. The false alarm rate (FAR = false alarms / (hits + false alarms)) is 6.7%.

For the TDWR comparison, Denver, CO (KFTG) was chosen because the coverage overlap between NEXRAD and TDWR is near optimal (the radars are roughly 7km apart). In addition, this environment is conducive for both wet and dry microbursts, which makes this site ideal for measuring AMDA performance for both categories.

Figure 5 shows a side by side comparison of NEXRAD and TDWR with AMDA and ITWS detections. In this case, the scan times were close (< 1 minute apart) and the agreement between the detections is high. In Figure 6, a time lapse of all detections observed over roughly a 1 hour time window is shown. The AMDA detections are shown in blue and ITWS in red. Overall detection placement is consistent between the two algorithms.

The results of the AMDA/ITWS comparison are shown in Figure 7. For this, 16 events were chosen for comparison. An "event" is a 2-3 hour window containing microburst-producing storms that fall in the overlap of AMDA and ITWS coverage. The fuzzy logic scoring method described in Section 3.2 was applied to both sets of detections. Despite the issues in comparing the output of the two algorithms, AMDA results appear to be comparable to ITWS results, with 85% of all ITWS microburst detections being matched to AMDA detections, and 89% of AMDA detections matched to ITWS detections.

The 85% probability of detection observed when using ITWS as "truth" is notably lower than the more optimistic 98.7% observed using human truth. We believe this degradation is due in part to three main causes: (i) more short lived microbursts have a higher chance of being detected by ITWS because of the higher scan rate of the TDWR; (ii) the increased range resolution of the TDWR yields stronger shear patterns in the radial velocity, especially in the case of dry microbursts and (iii) false alarms in ITWS will count as misses for AMDA, which negatively impact this score. In spite of these disadvantages, the results suggest that NEXRAD AMDA is a reliable tool for automated wind shear and microburst detection.

4. CONCLUSION

This work described the Automated Microburst Detection Algorithm (AMDA) that has been recently redesigned for NEXRAD. This algorithm will be integrated into the Open Radar Product Generator (ORPG) to provide automated wind shear and microburst detection for applications in meteorology and aviation safety.

AMDA generates wind shear detections by processing NEXRAD reflectivity and radial velocity scans. First, the AMDA Interest Generator uses image processing techniques to search for features and patterns in the inputs which are commonly observed in microbursts and other forms of wind shear. Next, shear segments are located, validated, and clustered to form regions of potential wind shear hazard. Regions that meet size and strength thresholds are output to the user in the form of a detection. Outputs are labeled into one of four wind shear categories depending on the size and strength of the event.

The validity of AMDA results was measured using two methods. First, a human observer searched NEXRAD data and identified wind shear events which were compared to AMDA output. Second, microburst detections obtained from the ITWS

system were compared to AMDA output in regions where the NEXRAD and TDWR overlap. The results of both comparison studies were positive, suggesting AMDA can provide reliable, automated wind shear detection to a large number of airports not supported by a TDWR.

Moving forward, there are a number of ways in which AMDA can be advanced. The NEXRAD Supplemental Adaptive Intra-volume Low-level scan (SAILS) provides an additional surface scan which can pick up short lived microbursts that might occur in between the current 4 minutes scan strategy used by NEXRAD. In addition, several more microburst precursors can potentially be derived from the recent dual pol upgrades applied to the NEXRAD network. In particular, hydrometeor classification (Smalley et al., 2009) can detect hail patterns which have been observed to be a microburst precursor in the DDPDA. There is also the possibility that these concepts can be used to add a predictive component to AMDA, but this remains a subject of future research.

References

Albo, D., 1994: Microburst detection using fuzzy logic. Report prepared for Terminal Area Surveillance System Program, NCAR Rep., 45 pp. [Available from David Albo, National Center for Atmospheric Research, 3450 Mitchell Lane, Boulder, CO 80301.]

Brown R. A. and Wood V. T., A Guide For Interpreting Doppler Velocity Patterns: Northern Hemisphere Edition. Available Online at http://www.nssl.noaa.gov/publications/dopplerguide/ [Accessed, 2013].

Dance, Sandy, and Rodney Potts. "Microburst detection using agent networks." Journal of atmospheric and oceanic technology 19.5 (2002): 646-653.

Delanoy, Richard L., Jacques G. Verly, and Dan E. Dudgeon. "Functional templates and their application to 3-D object recognition." Acoustics, Speech, and Signal Processing, 1992. ICASSP-92., 1992 IEEE International Conference on. Vol. 3. IEEE, 1992.

Evans, J., Ducot E., The Integrated Terminal Weather System (ITWS), MIT Lincoln Laboratory Journal, Volume 7, Number 2, 1994.

Fujita, Tetsuya Theodore. "Spearhead echo and downburst near the approach end of a John F. Kennedy Airport runway, New York City." SMRP Research Paper 137, University of Chicago, Illinois (1976).

Fujita, Tetsuya Theodore. "The Downburst: Microburst and Macroburst", SMRP Research Paper 210, University of Chicago, Illinois (1985).

Hallowell, Robert, et al. “Wind-Shear Cost Benefit Analysis Update”, Project Report ATC-341, MIT Lincoln Laboratory, 13 May 2009,

Jain, Michael, et al. "Software architecture of the NEXRAD open systems radar product generator (ORPG)." Aerospace and Electronics Conference, 1997. NAECON 1997., Proceedings of the IEEE 1997 National. Vol. 1. IEEE, 1997.

Johnson, J. T., P. L. MacKeen, A. Witt, E. D. Mitchell, G. J. Stumpf, M. D. Eilts, and K. W. Thomas, 1998: The Storm Cell Identification and Tracking algorithm: An enhanced WSR-88D algorithm. Wea. Forecasting, 13, 263–276.

Knupp, Kevin R. "Numerical simulation of low-level downdraft initiation within precipitating cumulonimbi: Some preliminary results." Monthly weather review 117.7 (1989): 1517-1529.

Newell, O.J. and J.A. Cullen, "ASR-9 Microburst Detection Algorithm," Lincoln Laboratory Project Report ATC-197, DOT/FAAINR-93-2, October 1993.

Smalley, D., et al. "Development of dual polarization aviation weather products for the FAA." AMS Conference Preprint. 2009.

Smith, Travis M., Kimberly L. Elmore, and Shannon A. Dulin. "A damaging downburst prediction and detection algorithm for the WSR-88D." Weather and forecasting 19.2 (2004): 240-250.

Trobec, J. Operational Difficulties Associated with Convective Wet Downbursts. 2006. Available online at http://www.jaytrobec.com/papers/ [Accessed, 2013].

Wilson, James W., et al. "Microburst wind structure and evaluation of Doppler radar for airport wind shear detection." Journal of climate and applied meteorology 23.6 (1984): 898-915.

Wolfson, M., Delanoy, R., Forman, B., Hallowell, R., Pawlak., M, Smith, P., Automated Microburst Wind-Shear Prediction, MIT Lincoln Laboratory Journal, Volume 7, Number 2, 1994.

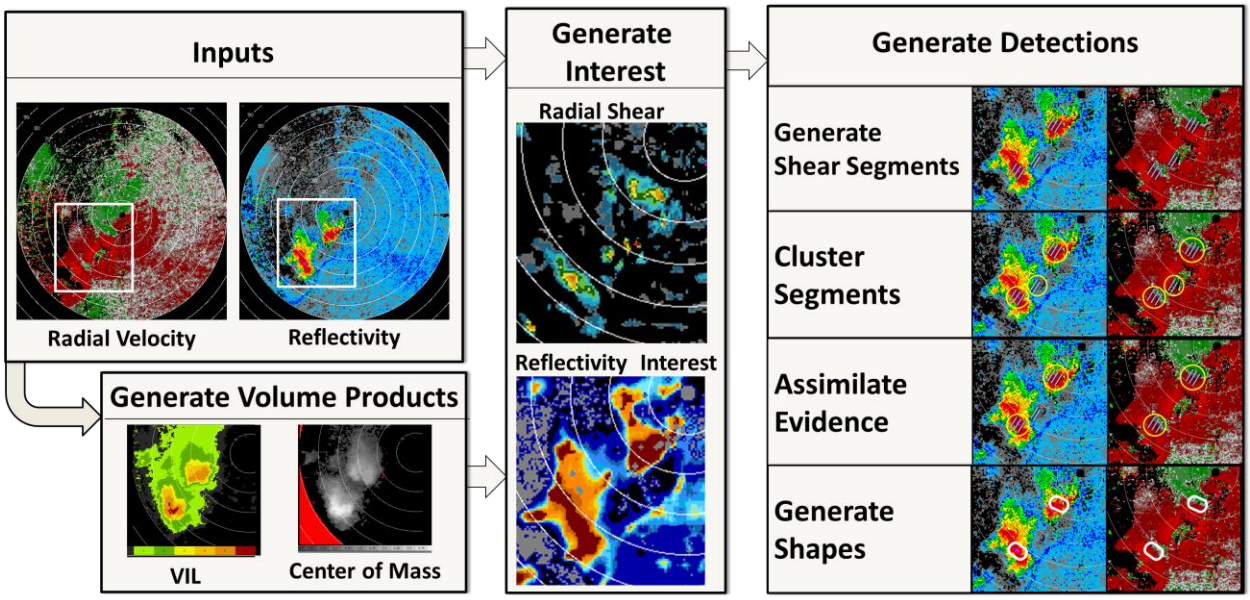

Figure 2: *AMDA Flow diagram. Elevations of Reflectivity and Radial Velocity are ingested as they become available. If volume products are required, all incoming elevations are sent to the Volume Product generator to create VIL and center of mass fields. Once base elevation data arrive, they are sent to the interest generator. The Interest Generator uses the base elevation products along with VIL and Center of mass to create the Radial Shear and Reflectivity Interest images. Shear segments are created from radial velocity and interest images, and are clustered. AMDA detections are created from clusters which meet a number of conditions (strong enough shear, size criteria, etc).*

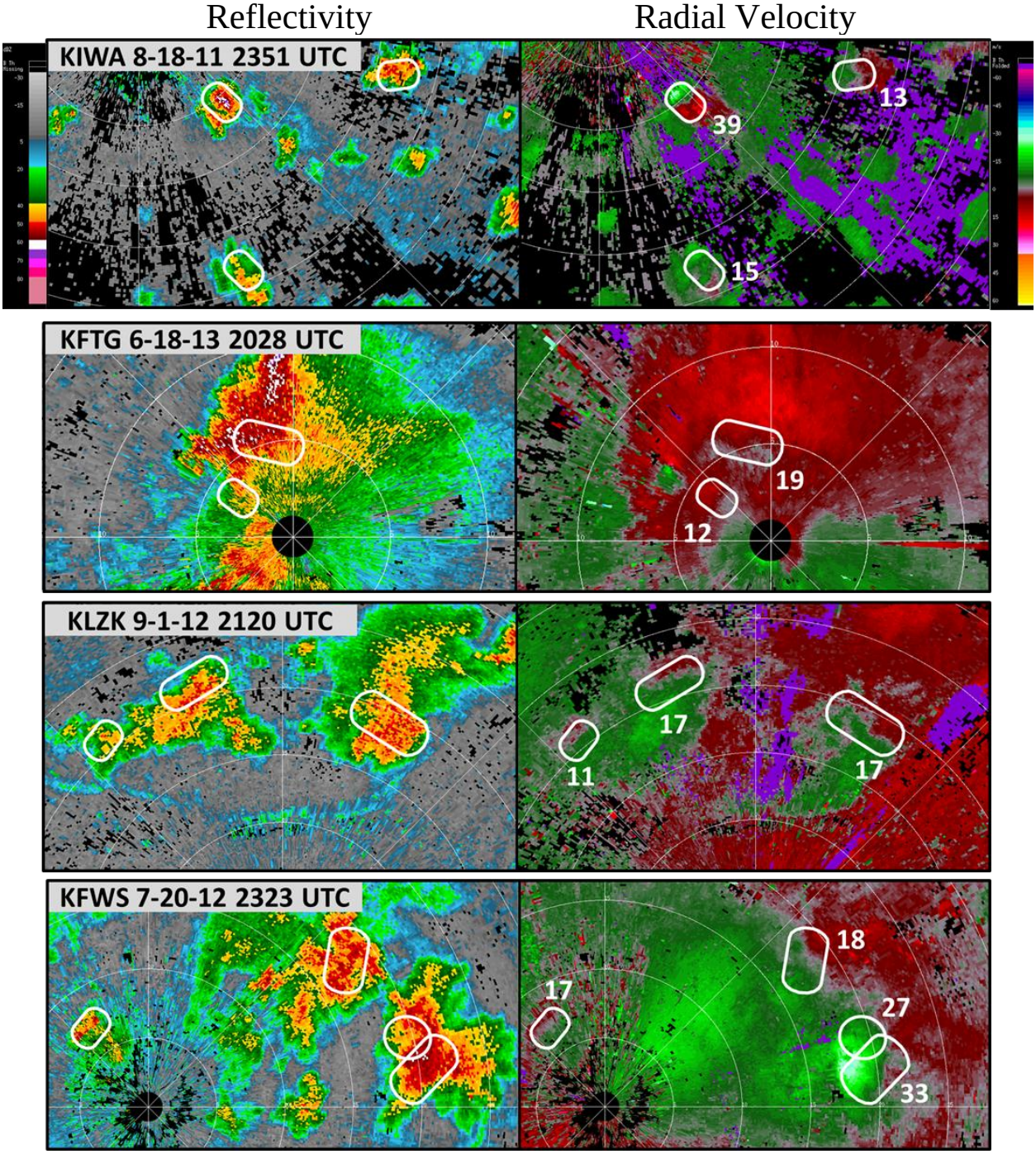

Figure 3: *Examples of AMDA output. Top: Two microbursts and weak wind shear detected in storms near KIWA (Phoenix, AZ) Second from Top: A large microburst (macroburst) detected east of a weak tornado near KFTG (Denver, CO). Third from Top: Two microbursts and wind-shear being tracked north of KLZK (Little Rock, AR) Bottom: Two macrobursts to the east and one microburst to the west of KFWS (Dallas/ Ft. Worth, TX). Notice that in this case the larger event is covered by overlapping detections.*

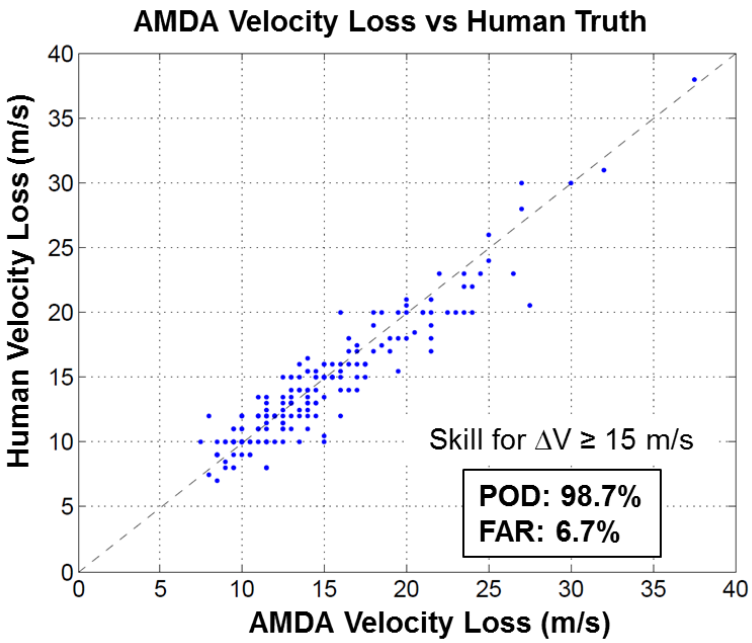

Figure 4: *Results of Human Truth scoring method. Shown is a comparison between the velocity loss (∆V) computed by AMDA vs the recorded velocity loss for matching truth detections identified by the human scorer. Unmatched AMDA and Human detections are not plotted, but are included in the Probability of Detection (POD) and False Alarm Rate (FAR) computed in the lower right. When computing POD and FAR, a 2m/s error margin was allowed for events with strength near 15 m/s.*

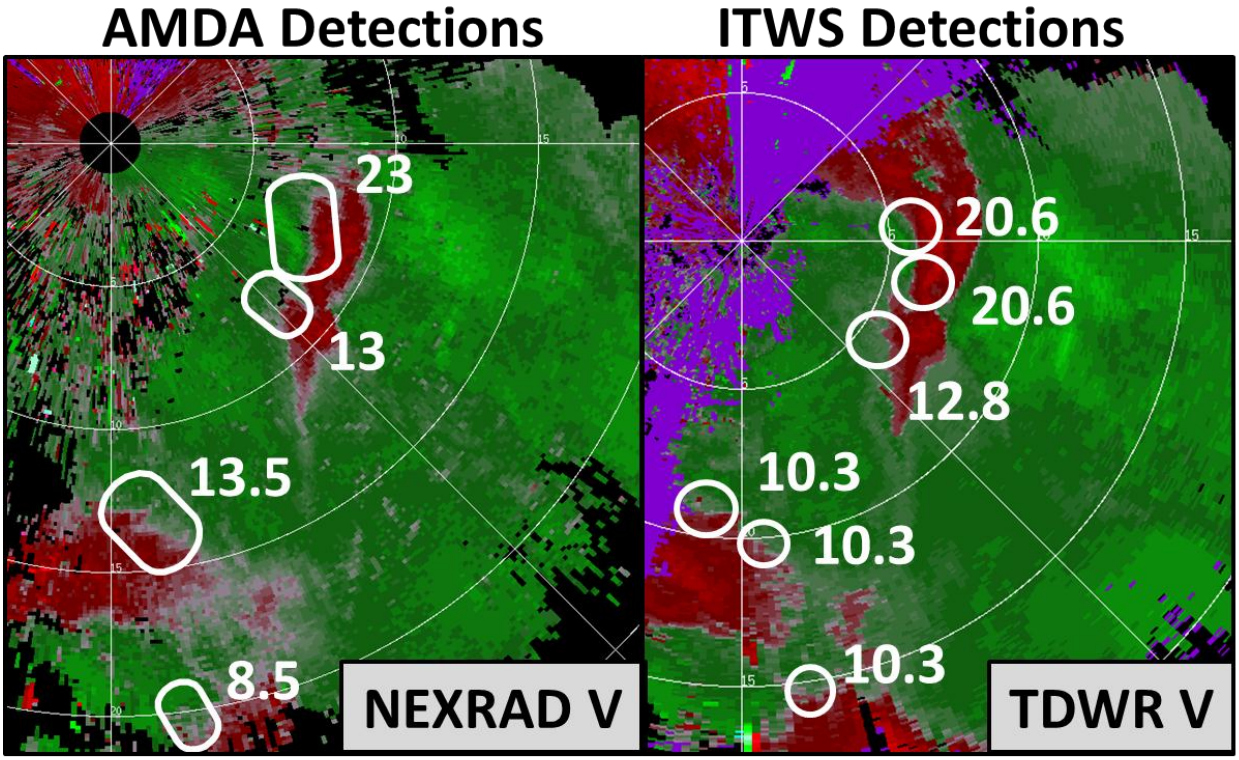

Figure 5: *Single time comparison of the KFTG NEXRAD AMDA (left) and Denver's TDWR ITWS (right). The microburst detections generated by both algorithms along with their strength are shown in white. In this case, both algorithms generated similar results, and both detected a large microburst south/southeast of both radars.*

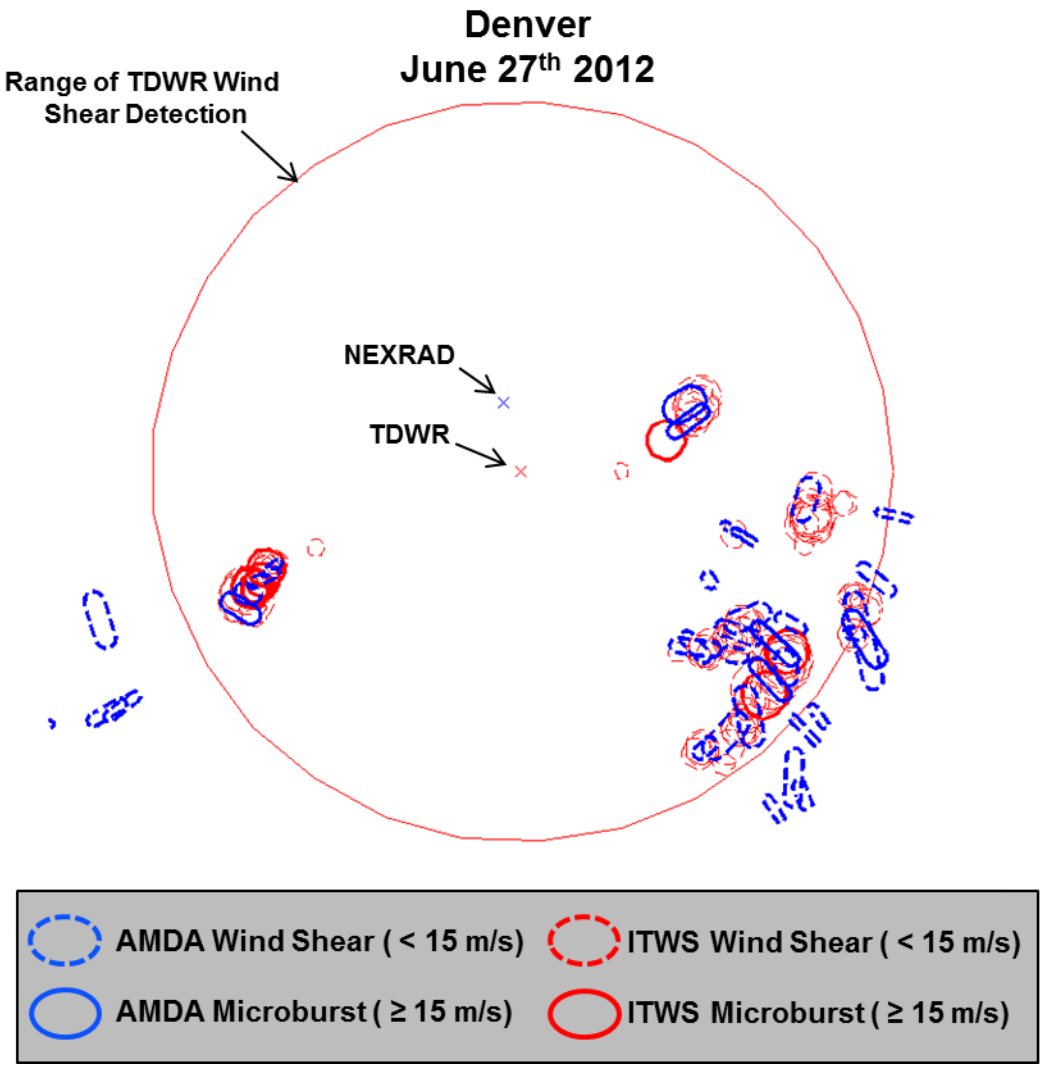

Figure 6: *A time lapse of approximately one hour of all AMDA and ITWS detections near Denver, CO. This case demonstrates that the size and location of the detections generated by both AMDA and ITWS are similar; however, ITWS shows a larger number because of the higher scan rate of the TDWR. The red ring denotes the 35 km range of the ITWS algorithm. Observe that AMDA runs with a larger range and shows a number of wind shear detections outside the range of ITWS.*

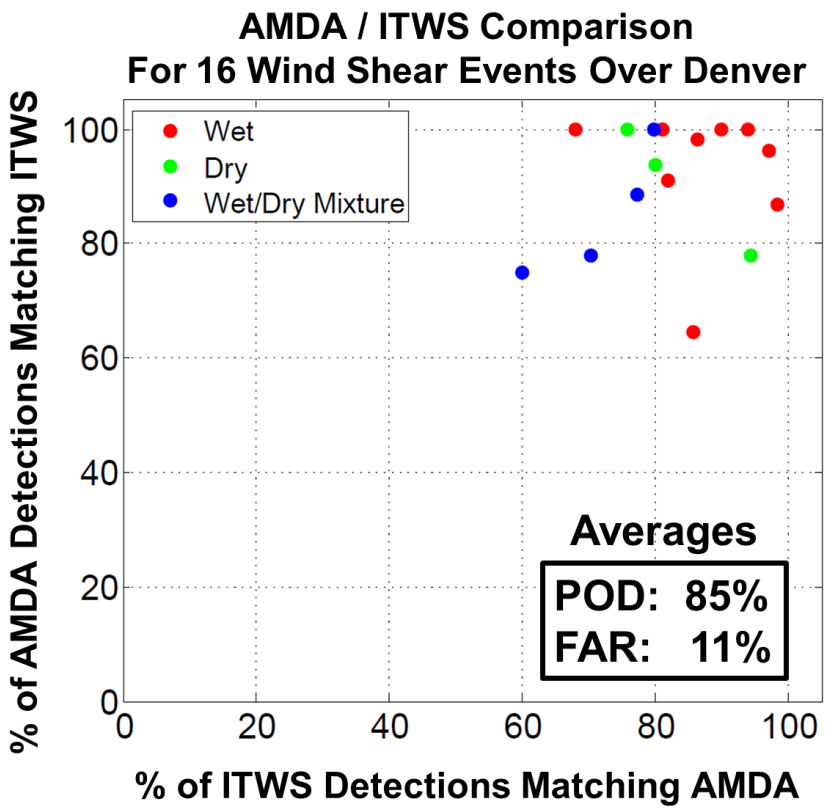

Figure 7: *A summary of AMDA vs ITWS results for 16 events near Denver, CO, where ITWS detections are considered as "Truth". Plotted are the percentage of AMDA detections that were matched to an ITWS detection, and the percentage of ITWS detections which were matched to an AMDA detection (the upper right corner of the plot represents perfect agreement). Each "event" consists of a 2-3 hour time window where severe wind shear impacted the region. Overall, there is agreement between the two types of detections. The events were further classified based on whether the recorded microbursts were "wet" or "dry" (this was determined by applying a threshold to the dBZ observed within these detections). These results suggest AMDA's performance is slightly worse for drier microbursts*